Volume 18 | Number 18 | 14 May 2016 | Pages 12379–13132

# PCCP

Physical Chemistry Chemical Physics

www.rsc.org/pccp

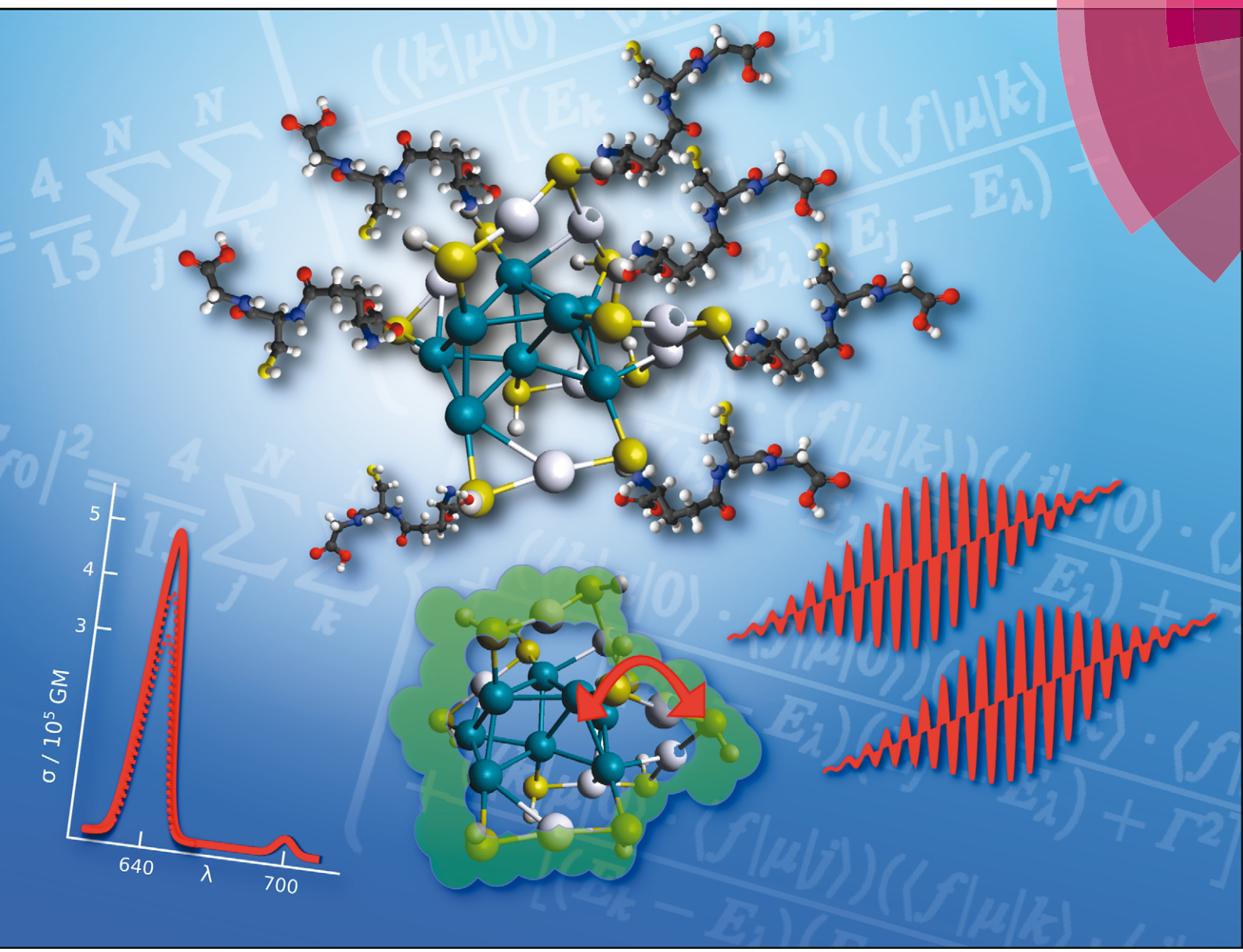


ISSN 1463-9076

ROYAL SOCIETY OF CHEMISTRY

COMMUNICATION

Rodolphe Antoine, Vlasta Bonačić-Koutecký *et al.*

Two-photon absorption of ligand-protected $Ag_{15}$ nanoclusters. Towards a new class of nonlinear optics nanomaterials

175 YEARS

PCCP

COMMUNICATION

View Article Online
View Journal | View Issue



Cite this: *Phys. Chem. Chem. Phys.*, 2016, **18**, 12404

Received 11th January 2016,
Accepted 20th January 2016

DOI: 10.1039/c6cp00207b

www.rsc.org/pccp

# Two-photon absorption of ligand-protected $Ag_{15}$ nanoclusters. Towards a new class of nonlinear optics nanomaterials†

Željka Sanader,[ab] Marjan Krstić,[a] Isabelle Russier-Antoine,[c] Franck Bertorelle,[c] Philippe Dugourd,[c] Pierre-François Brevet,[c] Rodolphe Antoine*[c] and Vlasta Bonačić-Koutecký*[ad]

**We report theoretical and experimental results on two-photon absorption (TPA) cross section of thiolated small silver cluster $Ag_{15}L_{11}$ exhibiting extraordinary large TPA in red. Our findings provide the responsible mechanism and allow proposing new classes of nanoclusters with large TPAs which are promising for biological and medical applications.**

Ligand protected noble metal clusters in the size regime smaller than ~1 nm exhibit remarkable quantum size effects.[1] In particular, their nonlinear optical (NLO) properties show extraordinary trends in the non-scalable size regime where each atom counts.[2–4] For instance, the two-photon absorption cross section for $Au_{25}$ in hexane is 427 000 GM at 800 nm, a value significantly larger than the typical value of approximately 1000 GM for organic macromolecules.[5] Also, it has been reported that water-soluble ssDNA-encapsulated Ag clusters exhibit large two-photon cross sections reaching 50 000 GM with high quantum yields in the red and near-IR part of the optical spectrum.[6] In spite of this, the elucidation of the fundamental photophysical mechanisms underlying two photon excited light emission from ligated nanoclusters with few noble metal atoms still requires an in-depth understanding of the structural and electronic interplay between the metallic and ligated parts of the clusters. The determination of the clusters structural properties is therefore the first step needed for the interpretation of the NLO experimental results. Structural properties for several ligated nanoclusters, mainly containing gold atoms, have thus been determined by single crystal X-ray crystallography.[7] Ligated clusters with 25 gold atoms have recently been reported to exhibit large two-photon absorption (TPA).[4,5] For such thiolated gold clusters $[Au_{25}(SH)_{18}]^{-1}$, which structure is known from crystallographic data,[8,9] TDDFT calculations have been used[10] to explain the large TPA cross sections that have been experimentally reported by Goodson and coworkers.[5] Calculated TPA cross sections within the three-states approximation were explained by resonance effects between one- and two-photon transitions. Besides, their values were shown to be strongly dependent on the choice of the X–C functional. Recently, one-photon absorption (OPA) properties of the smaller glutathione silver clusters $(Ag_{15}(SG)_{11})$[11] as well as the OPA and the NLO properties of the 15 gold atoms clusters $(Au_{15}SG_{13})$[7,11,12] exhibiting remarkable optical properties have been found. Two-photon absorption theory has been developed long time ago[13] but calculation of nonlinear properties of systems involving silver and gold subunits are more recent.[10,14,15] In this communication, we report TDDFT determined NLO properties of $Ag_{15}L_{11}$ (L = SH) with four confined electrons in the $Ag_8$ core. For this system, large fluorescence following OPA has been measured. Due to resonance effects, huge TPA cross sections in the red part of the spectrum are calculated while moderate TPA cross sections in the near-IR are predicted. This observation is in reasonable agreement with the measured TPA cross sections for the $Ag_{15}(SG)_{11}$ clusters, which are available in the range of 750–800 nm.

The two-photon absorption cross section for an excitation from the ground state $|0\rangle$ to a final state $|f\rangle$ is related to TPA transition probability for which the transition amplitude tensor has to be determined. For this purpose, we apply the quadratic response density functional theory QR-DFT using either single residue (SR) analytical formulation or *via* sum over states (SOS) method for which transition dipole moments are calculated within double residue QR method as described in Computational part, both in the framework of the DALTON quantum chemistry program.[19]

[a] *Center of excellence for Science and Technology-Integration of Mediterranean region (STIM) at Interdisciplinary Center for Advanced Sciences and Technology (ICAST), University of Split, Meštrovićevo šetalište 45, HR-21000 Split, Republic of Croatia*
[b] *Faculty of Science, University of Split, Teslina 12, HR-21000 Split, Republic of Croatia*
[c] *Institut Lumière Matière, UMR CNRS 5306 and Université Claude Bernard Lyon 1, Université de Lyon, 69622 Villeurbanne cedex, France. E-mail: rodolphe.antoine@univ-lyon1.fr*
[d] *Department of Chemistry, Humboldt Universitat zu Berlin, Brook-Taylor-Strasse 2, 12489 Berlin, Germany. E-mail: vbk@cms.hu-berlin.de*

† Electronic supplementary information (ESI) available: Analysis of transitions of one and two-photon absorption for $Ag_{15}SH_{11}$. Two-photon emission spectra at different pump powers for $Ag_{15}SG_{11}$. See DOI: 10.1039/c6cp00207b

We started with the structure of the $Ag_{15}L_{11}$ cluster (with L = $SCH_3$) containing an $Ag_8$ core which is protected by four ligands belonging to three different types.[11] In the present work, the ligand L has been further reduced to SH because the features of the one-photon absorption (OPA) spectrum remain almost unchanged.[11] Three types of ligands are present: $L_1$ (HS–Ag–SH), $L_2$ (HS–Ag–SH–Ag–SH) and $L_3$ type (HS–Ag–SH–Ag–SH–Ag–SH). The optimized structure of $Ag_{15}(SH)_{11}$ as well as the core with two $L_1$, and one $L_2$ and $L_3$ are shown in Fig. 1a.

The calculated and experimental one-photon absorption spectra of $Ag_{15}(SH)_{11}$ are given in Fig. 2. The analysis of the first four transitions (see Fig. S1 in ESI†) shows that these transitions arise from an excitation from the P-cluster-core orbital to the D-cluster-core-orbitals labelled by "core–core". $S_2$, $S_3$, $S_4$ transitions are located between 390 nm and 450 nm in good agreement with the position of the plateau observed in the experimental absorption spectrum (see Fig. 2).

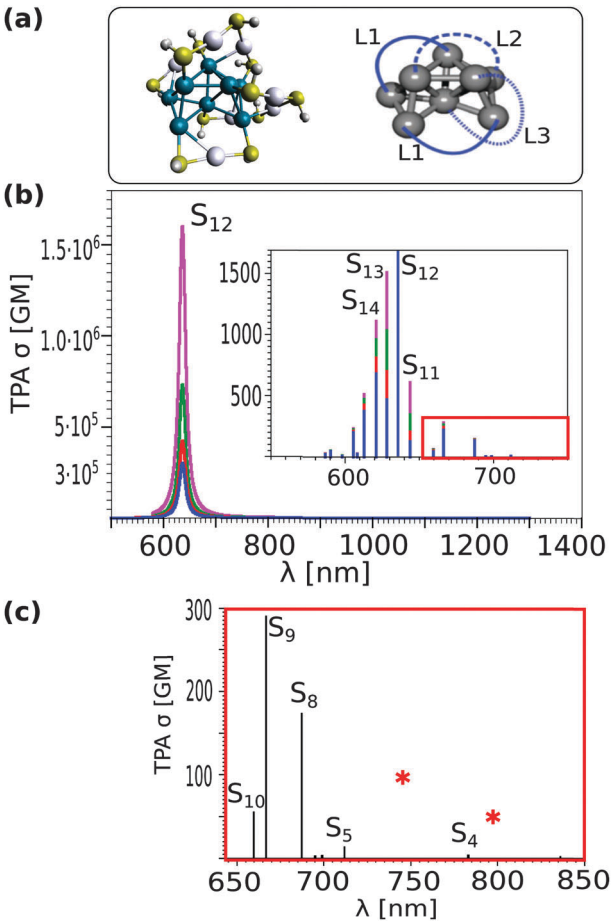


Fig. 1 (a) The lowest energy structure of $Ag_{15}L_{11}$ (with an $Ag_8$ core and staple ligands $L_n$ where n is the number of Ag atoms involved in the staple motif). (b) Two-photon absorption spectrum obtained with quadratic response QR-DFT method using sum over states (SOS) approach allowing to include a damping factor for each one photon transition ($\Gamma$ = 0.02, violet; $\Gamma$ = 0.03, green; $\Gamma$ = 0.04, red and $\Gamma$ = 0.05, blue). (c) Red asterisks are experimental TPA values reported in this work for $Ag_{15}(SG)_{11}$ compared with the single residue (SR) QR-DFT calculated values presented by black sticks.

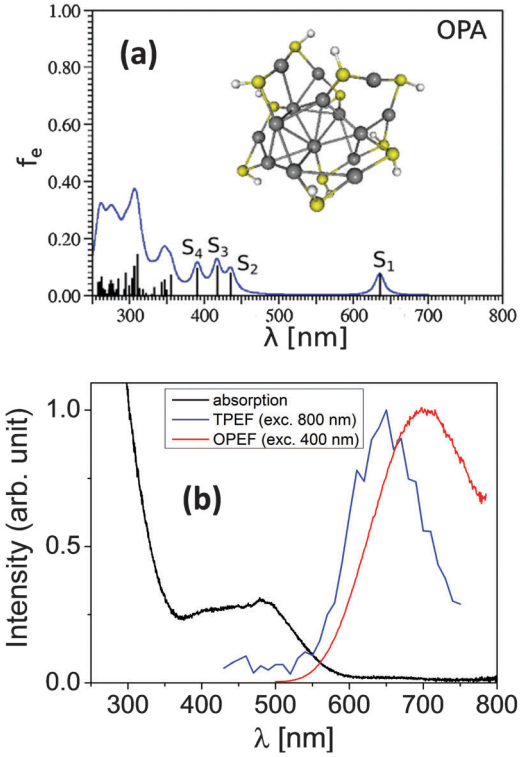


Fig. 2 (a) One-photon absorption spectrum for the lowest energy of $Ag_{15}(SH)_{11}$ obtained with TDDFT method using CAM-B3LYP functional and def2-TZVP basis set. (b) Spectroscopic characterization of the synthesized $Ag_{15}(SG)_{11}$ clusters dispersed in water. (top) Absorption (black), one photon excited (red) and two photon excited (blue) fluorescence spectra.

The two-photon absorption (TPA) spectrum for the optimized structure of $Ag_{15}L_{11}$ obtained with the quadratic response QR-DFT method using single residue (SR) (see Fig. 1c) and the sum over states (SOS) approach allowing to include a damping factor $\Gamma$ for each one photon transition is presented in Fig. 1b. Notice that the values of the cross sections calculated for $\Gamma = 0$ are identical with those obtained using single residue approach. A large resonance enhancement occurs when the excitation energy of an OPA state is close to half that of a TPA state. This is nicely illustrated in Fig. 3, with $S_1$ (630 nm) and $S_{12}$ (2 × 315 nm). In fact, the first excited state at 630 nm is in resonance with several states near 2 × 315 nm, resulting in an extremely large calculated TPA of over $10^6$ GM (see Fig. 1b). Note that the largest contributions to the sum-over states (see eqn (1)) are $\langle S_1|\mu|S_{12}\rangle$ = 23 D and $\langle S_{13}|\mu|S_{13}\rangle$ = 4 D. Indeed, the leading excitations corresponding to large TPA cross sections involve the ligands' orbitals and not only the core's ones (see Fig. S2 in ESI†). However, the absolute value of the cross section for TPA is found to be strongly dependent on the value of the damping factor. The choice of the $\Gamma$ values served to introduce corrections to TPA cross sections for more than two orders of magnitude as illustrated in Fig. 1b. For $\Gamma$ = 0.05 (*cf.* also ref. 10) the TPA cross section $\sigma$ is 300 000 GM. Indeed, the damping factor for two-photon transitions prevents the TPA cross section from blowing up near a one-photon resonance.

These results may have some features in common with π-organic molecules and in particular the stilbene derivative

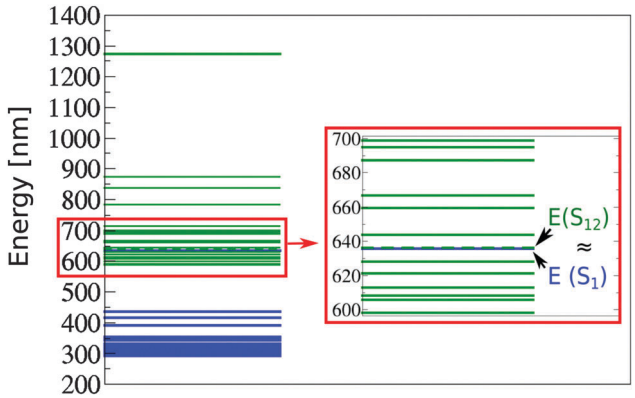


Fig. 3 Energies of one-photon OPA (blue) and two-photon TPA (green) states in nm illustrating the resonance between $S_1$ OPA and $S_{12}$ TPA excited states shown on right hand side.

(BDAS) with two π-donor groups (dibutyl amino group).[16] In BDAS, one of the largest changes occurs on the nitrogens, which are located at the opposite ends of the molecule. This change, coupled with the extended distance from the molecular origin results in a large transition dipole moment for this molecule, and thus leading to TPA about 20 times larger than the one reported for the molecule without the electron donor groups. In ligand protected silver nanoclusters, the central metal core may act as reservoir of delocalized electrons and the ligand surrounding the core may act as "donor groups". Upon excitation, ligand-to-core charge transfer (LCCT) or opposite core-to-ligand charge transfer (CLCT) might occur which is reflected in large transition dipole moments which has been obtained by calculations as mentioned above.

We attempted to determine the two-photon absorption and emission cross sections for these $Ag_{15}(SG)_{11}$ nanoclusters using the method reported in our previous work.[12] Experimentally, we found that the TPEF cross section at 800 nm excitation is 0.002 ± 0.0005 GM and the TPA cross section 69 GM. These experimental cross sections point to a quantum yield (QY = $\sigma_{TPE}/\sigma_{TPA}$) for $Ag_{15}(SG)_{11}$ nanoclusters of about $2.9 \times 10^{-5}$. At 750 nm, the TPA cross section increases up to 103 GM. These experimental values are in a good agreement with the calculated cross sections in this wavelength range using single residue approach (see Fig. 1c).

## Conclusions

In this communication, we report TDDFT calculations on the $Ag_{15}L_{11}$ (L = SH) clusters with four confined electrons in the $Ag_8$ core, for which a large one photon excited fluorescence has been observed. Due to resonance effects, huge TPA cross sections in the red part of the spectral region have been obtained within QR-TDDFT approach, while moderate TPA cross sections in near-IR have been calculated, in acceptable agreement with measured TPA cross sections of $Ag_{15}(SG)_{11}$ clusters. Exceptionally high TPA cross sections at long wavelength are expected when resonance between TPA and $S_1$ state of OPA occurs. The $S_1$ state is dominated by a HOMO–LUMO excitation. A low HOMO–LUMO gap is found in $Ag_{15}L_{11}$, indicating that $S_1$ is located in the red spectral range. The leading excitations in states with large TPA cross sections always involve ligands and not just the metal core. In ligand protected silver nanoclusters, the central metal core may act as reservoir of delocalized electrons whereas the ligands surrounding the core may act as the substituted groups, similarly to the BDAS case, where it acts as a donor, albeit in a 3D spatial frame. The above findings contain the key ingredients to propose new class of nanoclusters based NLO-phores with large TPA cross sections. The basic concepts presented here open a new route to control and tune the desired NLO properties for biological molecular reporters using silver nanoclusters.

## Computational

The structural and linear optical response properties corresponding to one-photon absorption (OPA) of $Ag_{15}L_{11}$ liganded clusters with L = SH have been determined using density functional theory (DFT) and its time-dependent version (TDDFT).[11,17]

For the silver atoms, the 19-e$^-$ relativistic effective core potential (19-e$^-$ RECP) from the Stuttgart group[18] taking into account scalar relativistic effects has been employed. For all atoms, triple zeta plus polarization atomic basis sets (TZVP) have been used.[18,19] The Perdew–Burke–Ernzerhof (PBE)[20] functional and Coulomb-attenuated version of Becke's three-parameter non-local exchange functional together with the Lee–Yang–Parr gradient-corrected correlation functional(CAM-B3LYP)[21] have been employed to determine the structural and OPA properties of $Ag_{15}L_{11}$, respectively.

For the two-photon absorption cross section the second order transition moments $S_{ab}$ can be identified from the single residue of the quadratic response function (see ref. 22 and 23 and reference therein). The two-photon absorption transition matrix from the ground state $|0\rangle$ to an excited state $|f\rangle$ can be written as a sum over state expression:

$$S_{ab} = \sum_k \left[ \frac{\langle 0|\hat{\mu}_a|k\rangle\langle k|\hat{\mu}_b|f\rangle}{\omega_k - \omega_f/2} + \frac{\langle 0|\hat{\mu}_b|k\rangle\langle k|\hat{\mu}_a|f\rangle}{\omega_k - \omega_f/2} \right] \quad (1)$$

where it is assumed that the frequency of the incident radiation is equal to half the excitation energy from the ground to the excited state, *i.e.* $\omega = \omega_f/2$. In the above equation $\mu_a$ and $\mu_b$ are the Cartesian components of the dipole moment operator $\mu$ and $\omega_k$ and $\omega_f$ are the frequencies of excitation from $|0\rangle$ to $|k\rangle$ and $|f\rangle$ respectively. In the case of linearly polarized light for an isotropic system, the two-photon absorption probability is defined as:

$$\langle \delta^{TPA} \rangle = \frac{1}{15} \sum_{ab} (S_{aa}S_{bb}^* + 2S_{ab}S_{ba}^*), \quad (2)$$

which can be converted to TPA cross section:

$$\sigma^{TPA} = \frac{(2\pi)^3 \alpha a_0^5 \omega^2}{c\pi L} \delta^{TPA} \quad (3)$$

where Lorentzian broadening with width $L = 0.1$ eV is used, $\alpha$ is the fine structure constant, $a_0$ is Bohr radius, $\omega$ is the energy of incoming photon and $c$ is the speed of the light.[24]

Alternatively, within the sum over states (SOS) approach for the case where both photons have the same energy $E_\lambda$, orientationally averaged expressions for the two-photon matrix elements for linearly polarized photons with parallel polarization two-photon matrix elements can be formulated as:

$$|S_{f0}|^2 = \frac{4}{15}\sum_j^N \sum_k^N \left\{ \begin{array}{l} \dfrac{(\langle k|\mu|0\rangle \cdot \langle f|\mu|k\rangle)(\langle j|\mu|0\rangle \cdot \langle f|\mu|j\rangle)}{\left[(E_k - E_\lambda)(E_j - E_\lambda) + \Gamma^2\right]} \\ + \dfrac{(\langle k|\mu|0\rangle \cdot \langle j|\mu|0\rangle)(\langle f|\mu|k\rangle \cdot \langle f|\mu|j\rangle)}{\left[(E_k - E_\lambda)(E_j - E_\lambda) + \Gamma^2\right]} \\ + \dfrac{(\langle k|\mu|0\rangle \cdot \langle f|\mu|j\rangle)(\langle f|\mu|k\rangle \cdot \langle j|\mu|0\rangle)}{\left[(E_k - E_\lambda)(E_j - E_\lambda) + \Gamma^2\right]} \end{array} \right\} \quad (4)$$

The damping factor $\Gamma$ for each one-photon transition serves to prevent the TPA cross section from blowing up near the one-photon resonances. For this reason, we adapted the SOS approach which requires explicit calculation of all transition dipole moments among excited states, as well as between them and the ground state which we realized in the framework of the double residue (DR) approach within DALTON program. This allowed us to adequately correct the TPA cross sections when necessary as well as to include manifold of states, usually 20 to 30 excited states avoiding ''few states'' model in which only the dominating terms in the two-photon absorption transition amplitude tensor are accounted for.[10] No influence of the truncation of the SOS from *e.g.* 20 to 15 states on the values of cross sections has been found. Notice that computational results should be considered as qualitative, since the influence of different functionals as well as inclusion of double excitations has not been investigated. Nevertheless, they can be used to illustrate the conceptual issues.

## Experimental

### Synthesis and characterization

$Ag_{15}(SG)_{11}$ nanoclusters were formed by reducing silver nitrate in the presence of excess glutathione, using a method that was similar to a previously reported method.[11] For characterization, PAGE separation was carried out by using a vertical gel electrophoresis unit with a size of 0.2 cm × 20 cm × 20 cm. The separating and stacking gels were prepared by acrylamide/bis-(acrylamide) monomers with the total contents of 35 wt% (acrylamide/bis-(acrylamide) 94 : 6), respectively. The eluting buffer consisted of 192 mM glycine and 25 mM tris(hydroxymethylamine). The as-prepared $Ag_{15}(SG)_{11}$ clusters were dissolved in a 15% (v/v) glycerol/water solution (6 mg in 100 μl). The samples solutions were loaded onto the stacking gel (10 μl per well) and eluted for 7 h at a constant voltage mode (150 V) to achieve sufficient separation. After gel separation, our synthesis leads to a major band closely located near the ''band 2'' in the Bigioni synthesis.[25,26]

### NLO experiments

The light source for the present two-photon absorption and emission experiments was a mode-locked femtosecond Ti:sapphire laser delivering at the fundamental wavelength of 800 nm pulses with a duration of about 140 femtoseconds at a repetition rate of 76 MHz. The beam was gently focused by a 5 cm focal length lens to a waist of 10 μm and sent in transmission into a 0.5 cm path length spectrophotometric cuvette. The transmitted light was detected with a large aperture photodiode. The incident power was controlled with a half-wave plate and a polarizing cube. The sample absorption, the concentration of which was set to 1 mM, was then determined as a function of the incident power. Such an experimental set-up is effectively a P-scan set-up. The calibration of the photodiode signal was obtained prior to the experiment by removing the cuvette and varying the incident power. The TPE light was collected at an angle of 90° from the incident direction by a 2.5 cm focal length lens. A short pass filter with a cut-off wavelength at 750 nm was placed before the monochromator to minimize the light scattering from the excitation beam (800 nm). Fig. S3 in ESI† shows the fluorescence spectra obtained after excitation at 800 nm and at different pump-powers for $Ag_{15}$ and pump-power dependence of the fluorescence which gave a slope of ~2 suggesting that it is indeed a two-photon excited emission.

## Note added in proof

After the submission of this paper we became aware of the recently published study, which reports a density functional theory (DFT) and time-dependent DFT (TDDFT) investigation on the linear and nonlinear optical response in silver nanoclusters.[27]

## Acknowledgements

The research leading to these results has received partial funding from the European Research Council under the European Union's Seventh Framework Programme (FP7/2007–2013 Grant agreement No. 320659). The authors also thank CNRS French-Croatian international lab (NCBA) for travel funding. VBK, ŽS and MK acknowledge funding from Center of Excellence (STIM).

## Notes and references

1 R. C. Jin, *Nanoscale*, 2010, **2**, 343–362.
2 R. Philip, P. Chantharasupawong, H. Qian, R. Jin and J. Thomas, *Nano Lett.*, 2012, **12**, 4661–4667.
3 S. Knoppe, H. Häkkinen and T. Verbiest, *J. Phys. Chem. C*, 2015, **119**, 27676–27682.
4 S. H. Yau, O. Varnavski and T. Goodson, *Acc. Chem. Res.*, 2013, **46**, 1506–1516.
5 G. Ramakrishna, O. Varnavski, J. Kim, D. Lee and T. Goodson, *J. Am. Chem. Soc.*, 2008, **130**, 5032–5033.
6 S. A. Patel, C. I. Richards, J.-C. Hsiang and R. M. Dickson, *J. Am. Chem. Soc.*, 2008, **130**, 11602–11603.
7 R. Hamouda, F. Bertorelle, D. Rayane, R. Antoine, M. Broyer and P. Dugourd, *Int. J. Mass Spectrom.*, 2013, **335**, 1–6.

8 M. W. Heaven, A. Dass, P. S. White, K. M. Holt and R. W. Murray, *J. Am. Chem. Soc.*, 2008, **130**, 3754–3755.
9 M. Zhu, C. M. Aikens, F. J. Hollander, G. C. Schatz and R. Jin, *J. Am. Chem. Soc.*, 2008, **130**, 5883–5885.
10 P. N. Day, K. A. Nguyen and R. Pachter, *J. Chem. Theory Comput.*, 2010, **6**, 2809–2821.
11 F. Bertorelle, R. Hamouda, D. Rayane, M. Broyer, R. Antoine, P. Dugourd, L. Gell, A. Kulesza, R. Mitrić and V. Bonačić-Koutecký, *Nanoscale*, 2013, **5**, 5637–5643.
12 I. Russier-Antoine, F. Bertorelle, M. Vojković, D. Rayane, E. Salmon, C. Jonin, P. Dugourd, R. Antoine and P.-F. Brevet, *Nanoscale*, 2014, **6**, 13572–13578.
13 S. H. Lin, Y. Fujimura, H. J. Neusser and E. W. Schlag, *Multiphoton spectroscopy of molecules*, Academic Press, Inc., 1984.
14 Z. Rinkevicius, J. Autschbach, A. Baev, M. Swihart, H. Ågren and P. N. Prasad, *J. Phys. Chem. A*, 2010, **114**, 7590–7594.
15 X. Li, Z. Rinkevicius and H. Ågren, *J. Chem. Theory Comput.*, 2014, **10**, 5630–5639.
16 M. Albota, D. Beljonne, J.-L. Brédas, J. E. Ehrlich, J.-Y. Fu, A. A. Heikal, S. E. Hess, T. Kogej, M. D. Levin, S. R. Marder, D. McCord-Maughon, J. W. Perry, H. Röckel, M. Rumi, G. Subramaniam, W. W. Webb, X.-L. Wu and C. Xu, *Science*, 1998, **281**, 1653–1656.
17 V. Bonačić-Koutecký, A. Kulesza, L. Gell, R. Mitrić, R. Antoine, F. Bertorelle, R. Hamouda, D. Rayane, M. Broyer, T. Tabarin and P. Dugourd, *Phys. Chem. Chem. Phys.*, 2012, **14**, 9282–9290.
18 D. Andrae, U. Haeussermann, M. Dolg, H. Stoll and H. Preuss, *Theor. Chim. Acta*, 1990, **77**, 123–141.
19 F. Weigend and R. Ahlrichs, *Phys. Chem. Chem. Phys.*, 2005, **7**, 3297–3305.
20 J. P. Perdew, K. Burke and M. Ernzerhof, *Phys. Rev. Lett.*, 1996, **77**, 3865–3868.
21 T. Yanai, D. P. Tew and N. C. Handy, *Chem. Phys. Lett.*, 2004, **393**, 51–57.
22 N. H. List, R. Zaleśny, N. A. Murugan, J. Kongsted, W. Bartkowiak and H. Ågren, *J. Chem. Theory Comput.*, 2015, **11**, 4182–4188.
23 P. Norman, *Phys. Chem. Chem. Phys.*, 2011, **13**, 20519–20535.
24 L. Frediani, Z. Rinkevicius and H. Ågren, *J. Chem. Phys.*, 2005, **122**, 244104.
25 J. Guo, S. Kumar, M. Bolan, A. Desireddy, T. P. Bigioni and W. P. Griffith, *Anal. Chem.*, 2012, **84**, 5304–5308.
26 S. Kumar, M. D. Bolan and T. P. Bigioni, *J. Am. Chem. Soc.*, 2010, **132**, 13141–13143.
27 P. N. Day, R. Pachter, K. A. Nguyen and T. P. Bigioni, *J. Phys. Chem. A*, 2016, DOI: 10.1021/acs.jpca.5b09623.

 